

AD-A199 702

DTIC FILE COPY

2

SACLANTCEN MEMORANDUM  
Serial No. 5M-211

**SACLANT UNDERSEA  
RESEARCH CENTRE**

**MEMORANDUM**



**Estimators for model-based  
passive localization**

E.J. Sullivan, W. Volkmann  
and S. Bongi

**DTIC  
ELECTE  
SEP 27 1988  
S D E**

July 1988

The SACLANT Undersea Research Centre provides the Supreme Allied Commander Atlantic (SACLANT) with scientific and technical assistance under the terms of its NATO charter, which entered into force on 1 February 1963. Without prejudice to this main task—and under the policy direction of SACLANT—the Centre also renders scientific and technical assistance to the individual NATO nations.

This document has been approved  
for public release and sale in  
distribution is unlimited.

88 9 27 128

---

This document is released to a NATO Government at the direction of SACLANT Undersea Research Centre subject to the following conditions:

- The recipient NATO Government agrees to use its best endeavours to ensure that the information herein disclosed, whether or not it bears a security classification, is not dealt with in any manner (a) contrary to the intent of the provisions of the Charter of the Centre, or (b) prejudicial to the rights of the owner thereof to obtain patent, copyright, or other like statutory protection therefor.
- If the technical information was originally released to the Centre by a NATO Government subject to restrictions clearly marked on this document the recipient NATO Government agrees to use its best endeavours to abide by the terms of the restrictions so imposed by the releasing Government.

---

Page count for SM-211  
(excluding covers)

---

Pages	Total
i-vi	6
1-8	8
01-08	8
	<hr/> 22

---

SACLANT Undersea Research Centre  
Viale San Bartolomeo 400  
19026 San Bartolomeo (SP), Italy

tel: 0187 540 111  
telex: 271148 SACENT I

NORTH ATLANTIC TREATY ORGANIZATION

SACLANTCEN SM-211

Estimators for model-based  
passive localization

E.J. Sullivan, W. Volkmann  
and S. Bongi

The content of this document pertains  
to work performed under Project 02 of  
the SACLANTCEN Programme of Work.  
The document has been approved for  
release by The Director, SACLANTCEN.



Issued by:  
Systems Research Division

  
J. Marchment  
Division Chief

Accession For	
NTIS GRA&I	<input checked="" type="checkbox"/>
DTIC TAB	<input type="checkbox"/>
Unannounced	<input type="checkbox"/>
Justification	
By _____	
Distribution/	
Availability Codes	
Dist	Avail and/or Special
A-1	

SACLANTCEN SM-211

- ii -

intentionally blank page

## SACLANTCEN EM-211

### Estimators for model-based passive localisation

E.J. Sullivan, W. Volkmann and S. Bongi

**Executive Summary:** Passive localisation techniques have not been really effective for many years and the aim of this SACLANTCEN work is an attempt to improve the situation. Preliminary results of this work have shown, for certain conditions, a radical improvement over the older basic methods but much work still remains to be done to show that the method remains robust in a variety of practical at-sea conditions.

The present 'standard' techniques of bearings-only and wavefront curvature make no use of available environmental information about the medium. Measurement of the multipath arrivals (ranging on the vertical) uses some of the medium information. However, the newer model-based (matched-field) passive ranging, as described in this memorandum, provides better localisation estimates by using all the available environmental information.

In this technique, a model is selected that describes the propagation channel to a reasonable degree and this is used to make a prediction of the field received at an array. This model field is then compared to the measured field and a set of source coordinates that provides the best match is taken as an estimate of the source position. This can be done in two ways: the problem can be inverted and one simply solves for the source coordinates or a search can be made over a prescribed set of possible source coordinates. For each set of source coordinates, an estimator is computed and used to select the best estimate of the coordinates.

This memorandum is a status report which studies the effect of four different types of estimator using both synthetic and real at-sea data. A comparison is made between Bucker's Estimator and three types of least-squares estimator. It is shown that Bucker's Estimator is, in general, inferior to the other three but it is recommended that further work with at-sea data is required before one can comment statistically on the optimum estimator.

SACLANTCEN 9M-211

- iv -

intentionally blank page

**Estimators for model-based passive  
localization**

E.J. Sullivan, W. Volkmann and S. Bongi

**Abstract:** A comparative study is made of the performance of four different estimators as used in the matched-field technique of passive localisation. The study is based on both real and synthesised data. In the synthesised data case, a comparison is made of the performance of the estimators for various signal-to-noise ratios. The four estimators studied are Bucker's Estimators, which can be thought of as a spatial matched filter, and three likelihood-type estimators. The results indicate that the matched-field type estimator has a slightly better signal-to-noise performance than the others, but rather poor sidelobe behaviour, whereas for the likelihood-type estimator the sidelobe behaviour is quite good.

**Keywords:** inverse problems,  $\sigma^2$  matched-field processing,  $\sigma^2$  model-based signal processing,  $\sigma^2$  passive localisation,  $\sigma^2$  passive ranging, hydroacoustics

underwater acoustics, Mediterranean Sea

SACLANTCEN SM-211

**Contents**

1. Introduction . . . . .	0
2. Theory . . . . .	0
3. Data characteristics . . . . .	0
4. Results . . . . .	0
5. Discussion . . . . .	0
References . . . . .	0



## 1. Introduction

Model-based passive ranging, sometimes referred to as *matched-field processing*, is basically an inverse problem. A propagation model that describes the propagation channel in some acceptable sense is selected, and is used to make a prediction of the field received on an array (usually, but not necessarily vertical). This model field is then compared to the measured field and the set of source coordinates that provide the best match to the measured field is then taken as the estimate of the source coordinates. This procedure can be carried out in two different ways. The problem can be directly inverted, solving for the source coordinates, or a search can be made over a prescribed set of source coordinates in some manner. For each set of source coordinates, an estimator is computed and used to select the best estimate of the coordinates. In the case of range-depth estimation, this estimator can be plotted on a range-depth map such that the estimates can be directly taken as the coordinates of some extremum. It is this technique that we are concerned with here. In particular, we make a comparative study of four different estimators based on both real and synthetic data. The estimators are Bucker's Estimator and three types of least-squares estimator. A thorough discussion of the subject of model-based passive localisation can be found in [1].

## 2. Theory

For the layered waveguide model with source on the  $z$  (or vertical) axis, the pressure field is symmetric about  $z$  and is therefore governed by the cylindrical wave equation which is given by

$$\frac{\partial^2}{\partial r^2} p(r, z, t) + \frac{1}{r} \frac{\partial}{\partial r} p(r, z, t) + \frac{\partial^2}{\partial z^2} p(r, z, t) = \frac{1}{c^2} \frac{\partial^2}{\partial t^2} p(r, z, t). \quad (1)$$

Since in this study a shallow-water range-independent scenario is chosen, Eq. (1) can be solved by separation of variables, since the range independence allows a factored form for the solutions. Assuming far-field conditions and a harmonic source (see [2] for details) the normal-mode model of Eq. (2) obtains:

$$p(r, z) = \sum_{m=1}^M \phi_m(z_0) \phi_m(z) \frac{e^{-\alpha_m r}}{\sqrt{k_m r}} e^{i k_m r}. \quad (2)$$

Here  $p$  is the acoustic pressure,  $\phi_m(z)$  is the  $m$ th modal function evaluated at  $z$ ,  $z_0$  is the source depth,  $r$  is the horizontal range,  $k_m$  is the horizontal wave number for the  $m$ th mode,  $\alpha_m$  is the loss factor for the  $m$ th mode, and  $M$  is the number of modes.

Assuming a vertical receiving array, Eq. (2) can be conveniently written in matrix form as

$$P_n = M_{n,m} \chi_m, \quad (3)$$

where  $P_n$  is the pressure at the  $n$ th hydrophone of the vertical receiving array with  $N$  hydrophones, and

$$M_{n,m} = \frac{\phi_m(z_n)}{\sqrt{k_m}},$$

$$\chi_m = \frac{\phi_m(z_0) e^{-(\alpha_m - i k_m) r}}{\sqrt{r}},$$

The estimation algorithm proceeds as follows:

- (1) Given the sound-velocity profile (SVP), the ocean depth and the bottom boundary conditions, compute  $\phi_m(z_n)$ ,  $\phi_m(z_0)$ ,  $k_m$  and  $\alpha_m$  for all desired values of  $z_0$ .
- (2) Compute the model pressure vector  $\{P_n^M(z_0, r)\}$  for a given set of values of  $r$  and  $z_0$ , from Eq. (3).

- (3) Compare  $\{P_n^M\}$  to the data vector  $\{P_n^D\}$  over the prescribed ranges of  $z_0$  and  $r$ .

It is the third step that we are concerned with here. Historically the estimator used for step 3 for the forward modelling procedure was based on the inner product of  $\{P_n^M\}$  and  $\{P_n^D\}$  [3]. This we will refer to as Bucker's Estimator. The form we use is written as

$$D_{BU} = \left| \sum_m P_m^D P_m^{M*} \right|^2 / (|P^D|^2 |P^M|^2), \quad (4)$$

where  $|P^D|^2$  and  $|P^M|^2$  are the squared magnitudes of the data and model vectors, respectively. We note that if one computes the expected value of  $D_{BU}$ , Eq. (4) becomes

$$\begin{aligned} \langle D_{BU} \rangle &= \left\langle \left( \sum_m P_m^D P_m^{M*} \right)^* \sum_l P_l^D P_l^{M*} \right\rangle \\ &= \sum_l \sum_m P_m^M \langle P_m^{D*} P_l^D \rangle P_l^{M*} \\ &= \sum_l \sum_m P_m^M R_{m,l} P_l^{M*}, \end{aligned} \quad (5)$$

where  $R_{m,l}$  is the covariance matrix of the data. In Eq. (5) the normalization has been ignored for simplicity; however in this study we will use the form expressed by Eq. (4). One then seeks the values of  $r$  and  $z_0$  that maximize  $D_{BU}$ .

The second estimator that we consider is the least squares fit of  $P^M$  to  $P^D$ , i.e. we seek the minimum of

$$D_{LS} = \sum_{m=1}^N |P_m^M - P_m^D|^2. \quad (6)$$

The data and model vectors are normalized to a reference hydrophone.

The third estimator is the incoherent form of  $D_{LS}$ . That is, we fit the hydrophone powers in a least-squares sense. Thus we seek the minimum of

$$D_{PW} = \sum_{m=1}^N (|P_m^M|^2 - |P_m^D|^2)^2. \quad (7)$$

The fourth estimator is based on an inversion of Eq. (3), and since this equation is linear in  $\chi_m$ , it can easily be solved by the method of least squares, under the assumption that  $N > M$ . This results in

$$\chi_l = [(M^M M)^{-1} M']_{l,n} P_n, \quad (8)$$

where  $M'$  is the transpose of  $M$ . The expression  $(M'M)^{-1}M'$  is sometimes referred to as the pseudo-inverse of  $M$ . Naturally, this reduces to  $M^{-1}$  when  $N = M$ . Equation (8) actually constitutes a modal filter, thus allowing modal selection in the solution. This turns out to be important in our case. The estimator we use for this approach is based on the least-squares fit of  $\chi_I$  to the prediction of  $\chi_I$  by the model. That is, we seek the minimum of

$$D_{ML} = \sum_{k=1}^K |\chi_I^M - \chi_I^P|^2, \quad (9)$$

where ML refers to maximum-likelihood in order to differentiate this estimator from  $D_{LS}$ , and  $K$  refers to the number of modes used. Here, as in the case of  $D_{LS}$ , the model and data vectors are normalized to a given complex amplitude.

### 3. Data characteristics

As mentioned in the introduction both real and synthetic data were used in this study. The synthetic data were generated by the SNAP model [4]. An ocean depth of 103 m was selected with a winter Mediterranean *sound velocity profile* (SVP). A point acoustic source of 190 Hz was taken to be at a depth of 50 m and a range of 7.4 km from the receiving array. This situation supported 9 modes. The receiver was a vertical array of 32 point hydrophones with a spacing of 2 m. The topmost hydrophone was located at a depth of 30 m. The bottom was composed of 2.5 m of sand over a rock sub-bottom. These complex synthetic data were then modified by the addition of a complex noise term that was taken from a random number generator with gaussian statistics. The signal-to-noise ratio at each hydrophone was taken to be equal.

The real data were taken at a depth of 103 m in the region north of the island of Elba in the Mediterranean. The SVP and bottom conditions were those used for the generation of the synthetic data. The source and receiver coordinates, as well as the frequency were also the same as for the synthetic data. The data were preprocessed by performing a 256-point FFT on a 2 s data record. The frequency line at 190 Hz was then taken as a 'snapshot' of the complex amplitude. The S/N ratio of these data was 30-40 dB.

Due to environmental conditions, mainly currents, the vertical array was not always vertical. Hence, it must be assumed that in the case of the real data, there are errors in the assumed positions of the hydrophones in the horizontal direction.

#### 4. Results

The four estimators were studied with regard to their performance under various S/N ratios in the case of the synthetic data, and also their performance with real data. Figures 1 through 3 depict the performance of  $D_{BU}$  for S/N ratios of 10, 20 and 30 dB respectively. Figure 4 gives the results of  $D_{BU}$  for real data. Figures 5 through 8 depict the same series of cases, i.e. 10, 20, 30 dB and real data, for  $D_{LS}$ . Continuing in this manner, Figs. 9 through 12 show the same four cases, respectively, for  $D_{PW}$  and finally, Figs. 13 through 16 present these same four cases for  $D_{ML}$ . As mentioned in Sect. 2, we seek the *maximum* of  $D_{BU}$  and the *minimum* of the other three estimators. However, in these illustrations, the likelihood surface has been inverted for  $D_{LS}$ ,  $D_{ML}$  and  $D_{PW}$  so that the extremum that we seek is the maximum in all four cases. This was done by dividing all values of the likelihood surface into its minimum value for these cases.

There are several conclusions that can be drawn from these figures. First, we see that  $D_{BU}$  suffers from a severe sidelobe problem, while at the same time has the best S/N performance. Although difficult to see due to the clutter caused by the sidelobes, the maximum of  $D_{BU}$  occurs at the correct position of  $r = 7.4$  km and  $d = 50$  m. In fact, this behaviour holds down to a S/N ratio of 0 dB (which is not shown). We note, however, that  $D_{BU}$  failed to indicate the solution in the case of the real data.

Considering next the behaviour of  $D_{LS}$ , we see that there is an immediate improvement in sidelobe performance, but the S/N performance is not quite as good since  $D_{LS}$  failed to provide a solution at S/N = 0 dB (which case is not shown). We also see that  $D_{LS}$  does not provide a solution for the real data case.

Continuing on to  $D_{PW}$ , we find the S/N performance slightly degraded with respect to that of  $D_{LS}$ , but there is a solution, although badly aliased, in the case of the real data. Although not obvious in the illustration, the peak at the correct coordinates of  $r = 7.4$  km and  $d = 50$  m is essentially equal to those at 13.5 km,  $d = 50$  m and  $r = 5.0$  km,  $d = 15$  m. Thus, the solution is not unique. It should be noted that the solution seems to be unbiased.

Proceeding to the last case, that of  $D_{ML}$ , we find that the S/N performance is even worse than that of  $D_{PW}$ . However, again there is a solution with the real data. It is biased in depth and, as can be clearly seen, there are two larger erroneous solutions. This solution was obtained by using only the first 7 modes in the solution. If more or less than 7 modes were used, no solution was obtained.

## 5. Discussion

Generally speaking the performance of  $D_{BU}$  seems to be inferior to the other three estimators. Although its S/N performance is better than that of any of the others, the sidelobe behaviour is so poor, that without a perfect match to the model one would expect this advantage to disappear rapidly, since a slight elevation of any of the aliased solutions would be disastrous. The sidelobe behaviour could be improved in two situations. First more modes tend to lower the sidelobes; therefore a scenario with higher frequency and/or deeper ocean depth could improve things. Secondly, the array data can be 'beamformed', i.e. can be passed through some preprocessing to provide more spatial selectivity. This is done in [4] where the so-called *maximum-likelihood* beamformer is used to preprocess the data.

Since the hydrophone positions were not well known due to the tilting of the vertical array, one suspects that the generally poor performance in the case of the real data is due to this 'mismatch' between the model and the true situation. Thus one could speculate that the phase errors produced by this mismatch are ignored by  $D_{PW}$ , which is essentially an incoherent version of  $D_{LS}$ . Thus at the expense of some S/N performance, robustness to mismatch is achieved by  $D_{PW}$ . This issue of mismatch enters into the case of  $D_{ML}$  also. Here, as pointed out above, a solution was obtainable only in the case of 7 modes. This suggests that the mismatch caused unacceptable errors in modes 8 and 9 and therefore the ability to filter them out is crucial to a coherent-type estimator.

A general conclusion then, is that array tilt is a serious problem and the level of seriousness can depend on the particular estimator that one uses. One way that such problems can be avoided is to eliminate the need for *a priori* knowledge of the model parameters. A means by which this can be done is given in [5] where it is shown that knowledge of the horizontal wavenumbers, which can be estimated with either a long towed array or a synthetic aperture towed array, is sufficient to estimate range. This could have important ramifications for these methods, since a recent study [6] has shown that mismatch in the environmental parameters can have serious deleterious effects.

Finally, it is worth mentioning that although the general S/N performance does not seem too promising, the synthetic data were not averaged. That is, the noise was directly added as a single realization of a gaussian process. This corresponds to a single 'snapshot' of real data with no time averaging. Thus the S/N values should be considered as a worst-case situation that would improve with averaging.

**References**

- [1] SULLIVAN, E.J. Passive localisation with propagation models. SACLANTCEN SR-117, La Spezia, Italy, SACLANT ASW Research Centre, 1987.
- [2] CLAY, C.S. and MEDWIN, H. *Acoustical Oceanography*, Wiley, New York, NY, 1977.
- [3] BUCKER, H.P. Use of calculated sound fields and matched-field detection to locate sound sources in shallow water. *Journal of the Acoustical Society of America*, **59**, 1976: 368-373.
- [4] BAGGEROER, A.B., KUPERMAN, W.A. and SCHMIDT, H. Matched field processing: source localization in correlated noise as an optimum parameter estimation problem. *Journal of the Acoustical Society of America*, **83**, 1988: 571-587.
- [5] CANDY, J.V. and SULLIVAN, E.J. Model-based passive ranging. Submitted to the *Journal of the Acoustical Society of America*.
- [6] HAMSON, R.M. and HEITMEYER, R.M. An analytical study of the effects of environmental and system parameters on source localisation in shallow water by matched field processing of a vertical array. SACLANTCEN Report, in preparation.



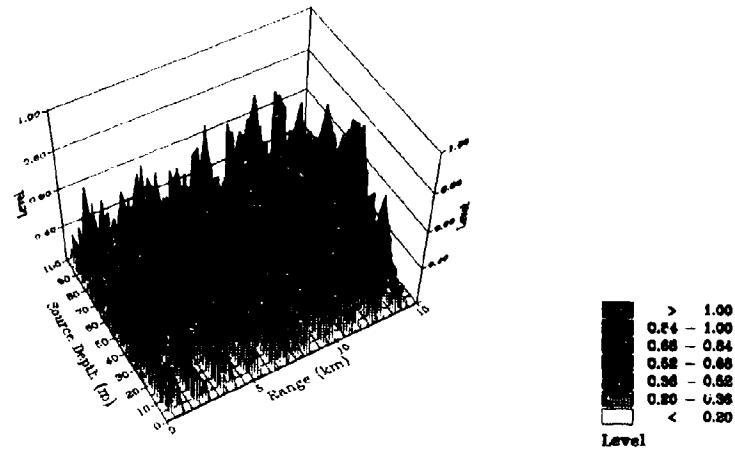


Fig. 1. Contour plot of Bucker's Estimator for the case of synthetic data with a signal-to-noise ratio of 10 dB.

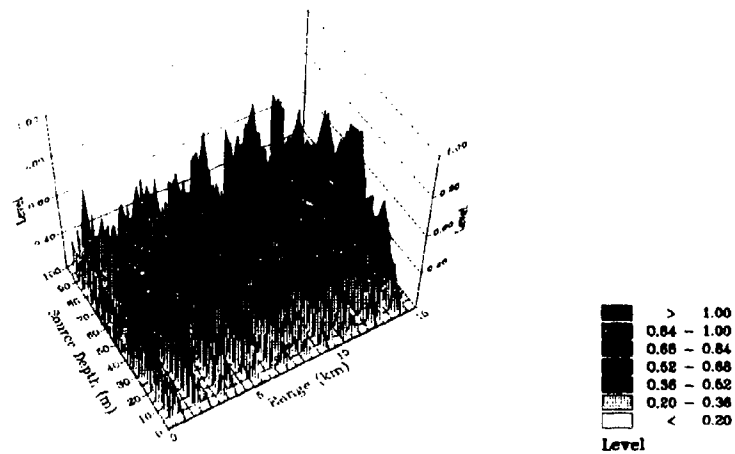


Fig. 2. Contour plot of Bucker's Estimator for the case of synthetic data with a signal-to-noise ratio of 20 dB.

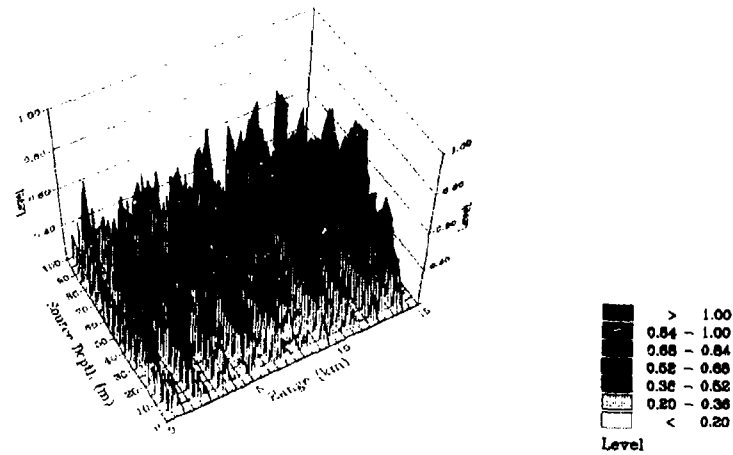


Fig. 3. Contour plot of Bucker's Estimator for the case of synthetic data with a signal-to-noise ratio of 30 dB.

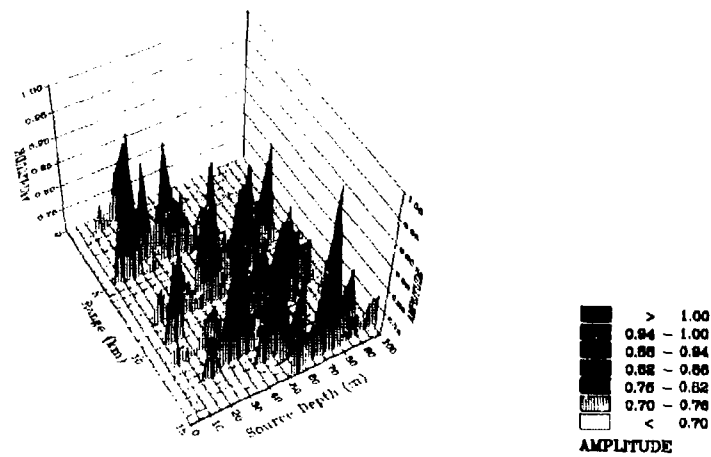


Fig. 4. Contour plot of Bucker's Estimator for the case of real data.

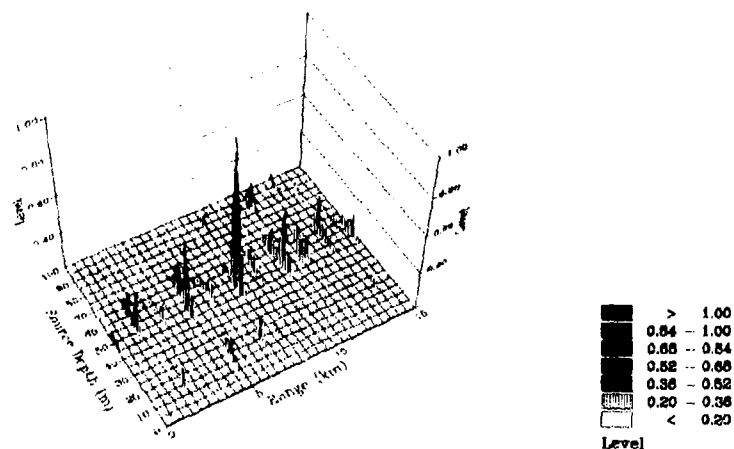


Fig. 5. Contour plot of the mean-squared error of the pressure field for the case of 10 dB signal-to-noise ratio. The data are inverted such that the maximum of the plot corresponds to the minimum mean-squared error.

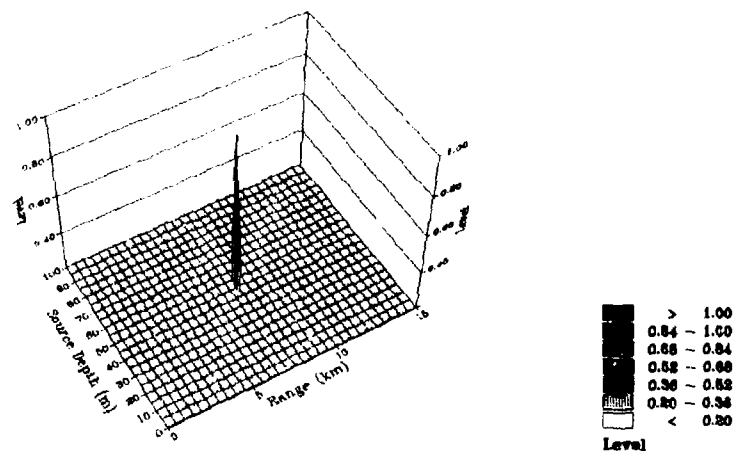


Fig. 6. Contour plot of the mean-squared error of the pressure field for the case of 20 dB signal-to-noise ratio. The data are inverted such that the maximum of the plot corresponds to the minimum mean-squared error.

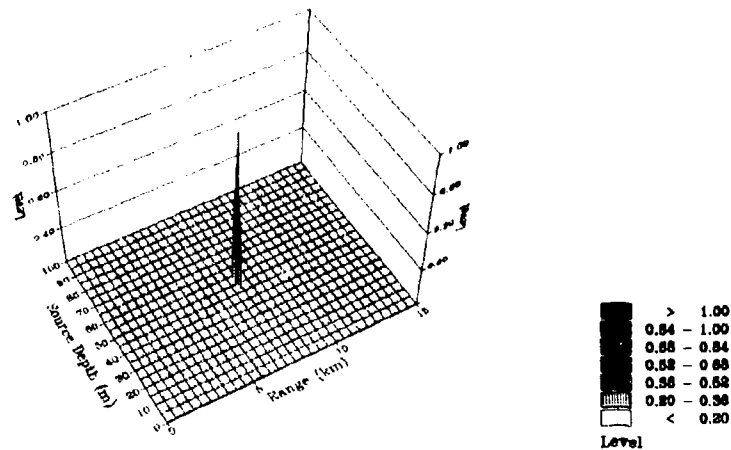


Fig. 7. Contour plot of the mean-squared error of the pressure field for the case of 30 dB signal-to-noise ratio. The data are inverted such that the maximum of the plot corresponds to the minimum mean-squared error.

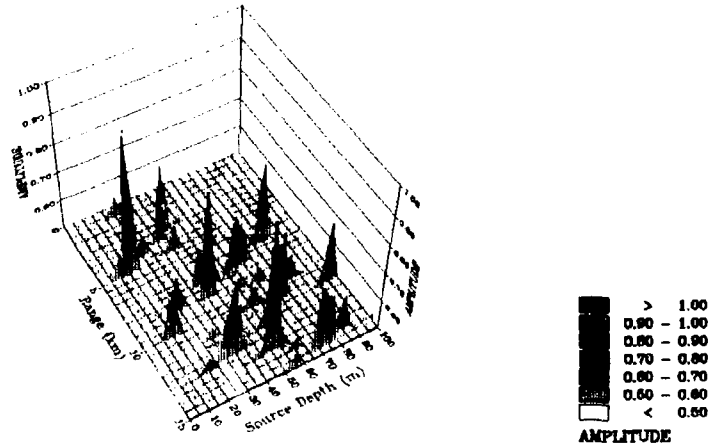


Fig. 8. Contour plot of the mean-squared error of the pressure field for the case of real data. The data are inverted such that the maximum of the plot corresponds to the minimum mean-squared error.

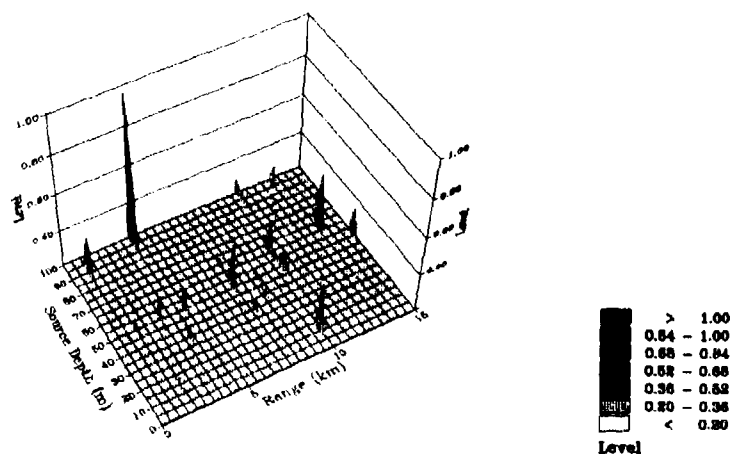


Fig. 9. Contour plot of the mean-squared error of the hydrophone power for the case of synthetic data with signal-to-noise ratio of 10 dB. The data are inverted such that the maximum of the plot corresponds to the minimum mean-squared error.

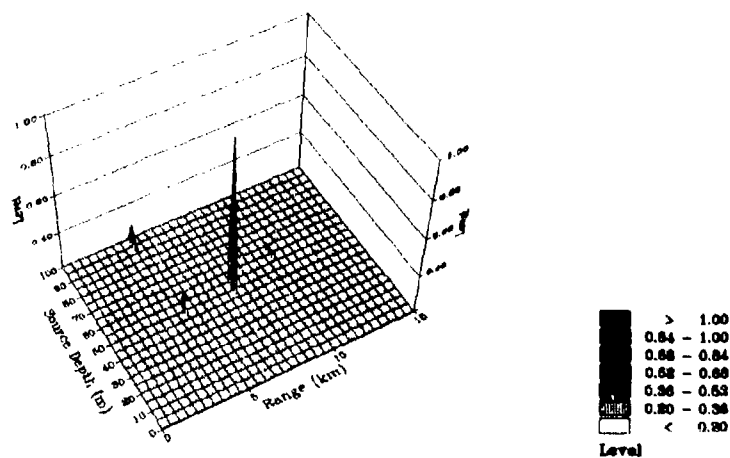


Fig. 10. Contour plot of the mean-squared error of the hydrophone power for the case of synthetic data with signal-to-noise ratio of 20 dB. The data are inverted such that the maximum of the plot corresponds to the minimum mean-squared error.

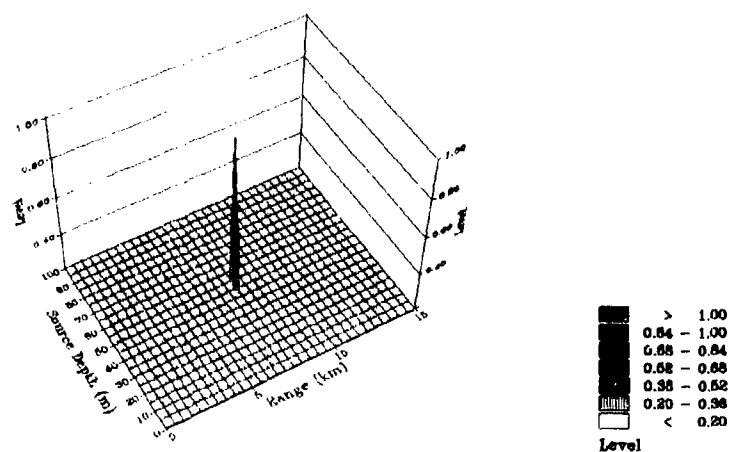


Fig. 11. Contour plot of the mean-squared error of the hydrophone power for the case of synthetic data with signal-to-noise ratio of 30 dB. The data are inverted such that the maximum of the plot corresponds to the minimum mean-squared error.

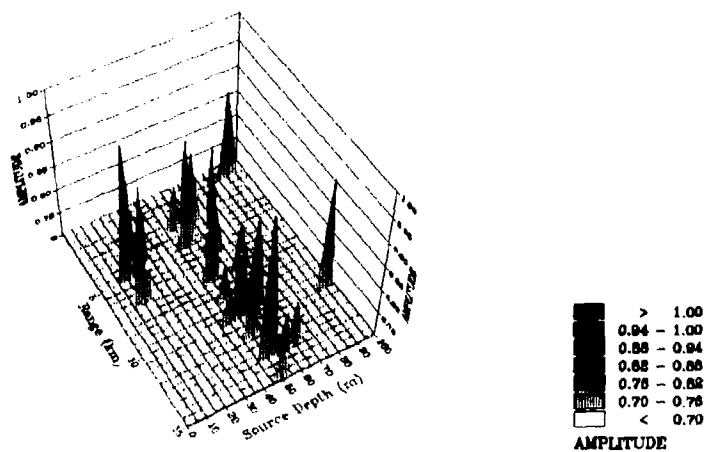


Fig. 12. Contour plot of the mean-squared error of the hydrophone power for the case of real data. The data are inverted such that the maximum of the plot corresponds to the minimum mean-squared error.

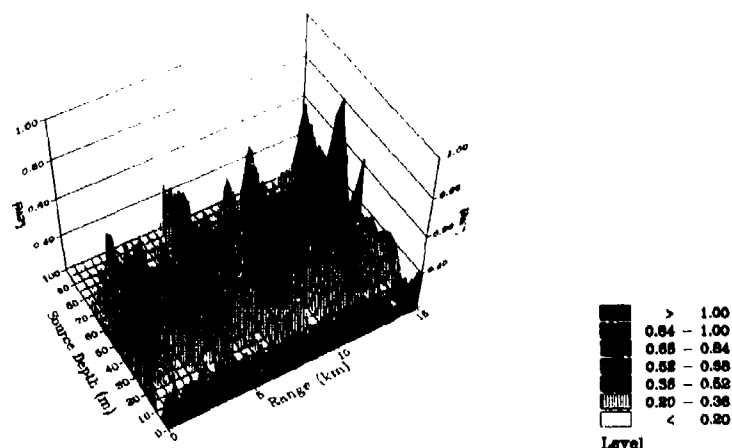


Fig. 13. Contour plot of the mean-squared error of the modal amplitudes for the case of synthetic data with signal-to-noise ratio of 10 dB. The data are inverted such that the maximum of the plot corresponds to the minimum mean-squared error.

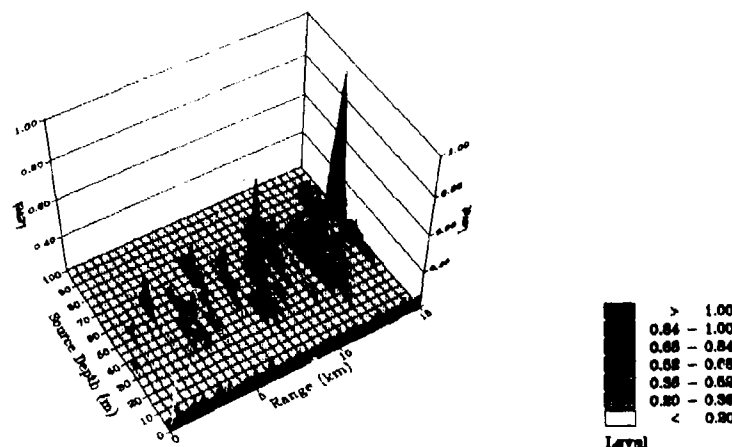


Fig. 14. Contour plot of the mean-squared error of the modal amplitudes for the case of synthetic data with signal-to-noise ratio of 20 dB. The data are inverted such that the maximum of the plot corresponds to the minimum mean-squared error.

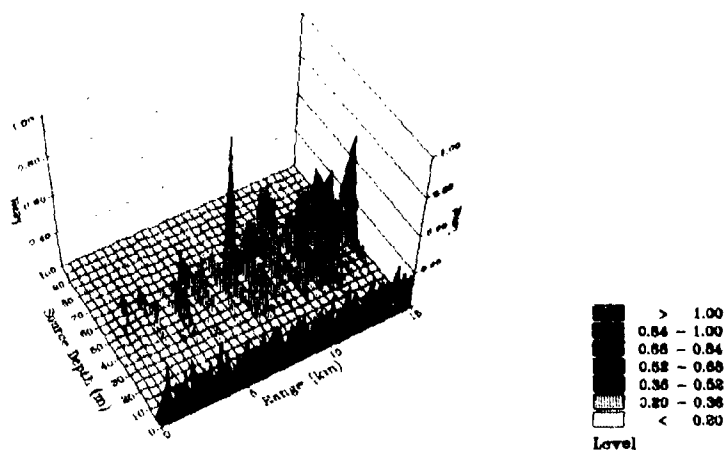


Fig. 15. Contour plot of the mean-squared error of the modal amplitudes for the case of synthetic data with signal-to-noise ratio of 30 dB. The data are inverted such that the maximum of the plot corresponds to the minimum mean-squared error.

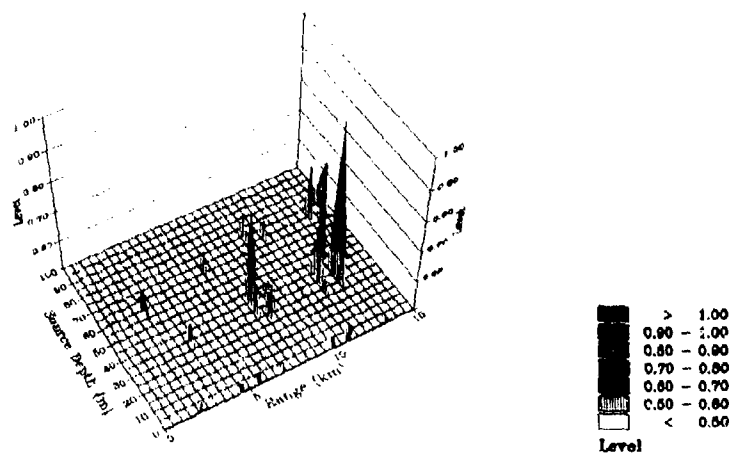


Fig. 16. Contour plot of the mean-squared error of the modal amplitudes for the case of real data. The data are inverted such that the maximum of the plot corresponds to the minimum mean-squared error.



# Initial Distribution for SM-211

## Ministries of Defence

JSPHQ Belgium	2
DND Canada	10
CHOD Denmark	8
MOD France	8
MOD Germany	15
MOD Greece	11
MOD Italy	10
MOD Netherlands	12
CHOD Norway	10
MOD Portugal	2
MOD Spain	2
MOD Turkey	5
MOD UK	20
SECDEF US	68

## NATO Authorities

Defence Planning Committee	3
NAMILCOM	2
SACLANT	3
SACLANTREPEUR	1
CINCWESTLANT/	
COMOCEANLANT	1
COMSTRIKFLTANT	1
CINCIBERLANT	1
CINCEASTLANT	1
COMSUBACLANT	1
COMMAIREASTLANT	1
SACEUR	2
CINCNORTH	1
CINCSOUTH	1
COMNAVSOUTH	1
COMSTRIKFORSOUTH	1
COMEDCENT	1
COMMARAIRED	1
CINCHAN	3

## SCNR for SACLANTCEN

SCNR Belgium	1
SCNR Canada	1
SCNR Denmark	1

SCNR Germany	1
SCNR Greece	1
SCNR Italy	1
SCNR Netherlands	1
SCNR Norway	1
SCNR Portugal	1
SCNR Turkey	1
SCNR UK	1
SCNR US	2
SECGEN Rep. SCNR	1
NAMILCOM Rep. SCNR	1

## National Liaison Officers

NLO Canada	1
NLO Denmark	1
NLO Germany	1
NLO Italy	1
NLO UK	1
NLO US	1

## NLR to SACLANT

NLR Belgium	1
NLR Canada	1
NLR Denmark	1
NLR Germany	1
NLR Greece	1
NLR Italy	1
NLR Netherlands	1
NLR Norway	1
NLR Portugal	1
NLR Turkey	1
NLR UK	1

Total external distribution	241
SACLANTCEN Library	10
Stock	29
Total number of copies	280